Eliminating the Interference of the Windshield Wipers on Lane Detection

Roopmeet Kaur[1*], Don-Gey Liu[2] and Chin-Hwa Cheng[3]

[1]Academy of Innovative Semiconductor and Sustainable Manufacturing, National Cheng Kung University, Taiwan
[2, 3]Department of Electrical Engineering, Feng Chia University, Taiwan
[1]Roopmeetkhurrana03@gmail.com
[2]dgliu@fcu.edu.tw, [3]chengch@fcu.edu.tw

Abstract. It's well developed in lane detection techniques for autonomous driving in advanced driver-assistance systems (ADAS). While keeping the vehicle localized in the correct track by detecting lane borders, interference may be caused by the windshield wipers, especially in bad weather conditions. Such annoyance may substantially deteriorate the accuracy of lane detection algorithms.

In this paper, an enhanced vision-based detection was investigated to mitigate the interference from the wipers. In this study, the wiper eliminating method was integrated as the preprocess with our lane detection algorithms. There were two algorithms employed in this study: the Sliding Window and the Hough Transform. Both algorithms employed the same image processing steps, which included image thresholding, Gaussian blurring, and Canny edge detection, to enhance lane features over noise. In addition, a region of interest (ROI) was established to segment the relevant road portions to ignore unwanted areas in each video frame. The accuracy and robustness were estimated to evaluate the profits of our wiper elimination process. A video in rainy conditions was used for testing. Experimental results showed a superior performance in the accuracy of lane detection and reliability, even in rainy conditions. The accuracy of Intersection of Union (IOU) was improved to 76.8%. It is promising that our wiper eliminating process will be easily included in the real-world ADAS.

Keywords: ADAS, Autonomous Self-Driving, Lane Detection, Sliding Window, Hough Transform, Wiper Interference.

1 INTRODUCTION

HIGH-precision Lane Detection is the foundation upon which innovative ADAS and autonomous driving technologies are built [1]. It supports fundamental functionalities like lane keeping and lane departure warnings, as well as prudent path planning. Extensive progress has been made so far on the design of robust computer vision-based lane detection systems for perfect driving conditions. However, these systems are ineffective for difficult driving conditions such as rain, snow, fog, and low-illumination conditions [2]. While driving conditions are difficult, road visual effects are degraded due to limited illumination, occluded road markings, road reflective, and water pools, which

B. Singh et al. (eds.), *Proceedings of the International Conference on Advances in Computing Technology and Artificial Intelligence (COMPUTATIA 2026)*, Atlantis Highlights in Intelligent Systems 18,
https://doi.org/10.2991/978-94-6239-713-2_48

heavily undermine traditional algorithms' reliability. Among all challenges posed by extreme weather conditions, windshield wipers are less focused yet as one of the highly disruptive factors for lane detection [3]. During rainy weather, wipers move periodically across the camera's field of view (FOV) to clear the windshield. This motion introduces dynamic artefacts, typically long, high-contrast lines, closely resembling lane markings in geometry and intensity. These false features are often detected by standard edge-based methods, such as Canny edge detection in OpenCV library, and falsely classified as lane lines by post-processing algorithms like the Hough Transform [3-1, 3-2] or sliding window techniques [3-3]. Furthermore, the rapid, sweeping motion of the wipers temporarily occludes actual lane markings, causing discontinuities in detection and further reducing the overall reliability of the system [4]. This interference is especially problematic in vision-only ADAS systems, where wiper edges may be mistaken for lane boundaries in multiple consecutive frames, leading to an erratic vehicle behavior, incorrect path planning, or even lane departure. Despite the importance of this issue, windshield wiper interference remains a relatively under-addressed problem in the current research landscape. While some studies have explored lane detection under general rainy or snowy conditions, few have noticed issues that explicitly handle wiper-induced occlusions and artefacts. Therefore, there is a need for real-time-capable techniques that can discriminate between actual lane markings and transient, wiper-related features.

Lee et al. addressed the challenge of lane detection under visually obstructive conditions, including the obstruction posed by windshield wipers [5]. They proposed an efficient approach for lane detection to perform effectively in an array of adverse driving situations, such as in rain, in low-light conditions, or in cases where windshield wipers and rain droplets blocked the camera images in its visibility. In the study in Ref. [5], the accuracy as well as the stability in lane detection was improved by integrating conventional algorithms with a new filtering process. In that study, a multistep pipeline system was employed through the processes from the noise reduction in the beginning to the enhancement of contrast. Bilateral filtering was utilized in reducing noises while retaining their edges. In addition, an adaptive contrast-enhancing multiscale retinex (MSR) was proposed to enhance the contrast dynamically depending on image frames in day or night times. In particular, there is an additional restriction step in Lee's system to remove false-positive lines that do not represent real lane markers. This restriction step operated by applying geometric constraints based on the orientation and distance of detected lines from the center of the camera image. This process can effectively eliminate fake lane marks in scenarios where windshield wipers cause false edges within the camera's FOV.

In analyzing the performance under the interference of the wipers, the authors included the case where the camera was occluded by oscillating windshield wipers. There were 100 images used for testing in that case. Detections of the left and right lane marks were assessed separately. The IOU values were evaluated for both left and right lane marks. In their study, the IOU scores achieved up to 65% for the left lane border and 69% for the right one. In their study, in addition to the conventional method by using Canny edge detection followed by Hough transform, two additional neural networks, DSUNet (a depth-wise separable U-Net variant) and U-Net ConvLSTM (a recurrent U-Net-based segmentation model with temporal memory), were proposed to replace

Hough transform to improve the resulted IOU data. In Ref. [5], the obtained IOU scores by the conventional method for the worst case were 49% and 40% for left and right marks, respectively. This fact reflects difficulty in removing wiper-induced interference. Even with the help of the proposed U-Net ConvLSTM, the obtained IOU values were improved to be 57% for the left mark and 54% for the right one. The performance by DSUNet was the best in the three methods. The achieved IOU values for the left and the right marks were 72% and 63%, respectively.

From all approaches tested, the presented system was the most resilient against the visual interference induced from the moving wipers. And a good performance was achieved in terms of detecting both sides under adverse situations [5]. In this paper, a systematic exploration and resolution of this problem is introduced by enhancing two popular traditional methods: the Sliding Window approach and the Hough Transform method. By incorporating pre-processing techniques like adaptive thresholding, median filtering, and geometric constraints, we show that even conventional techniques, carefully modified, can preserve lane detection performance even under conditions of wiper interference and rainy weather conditions. We verified our methods using quantitative measures such as IOU and frame-by-frame comparisons and demonstrated substantial improvement in detection precision and consistency.

2 VIDEO DATA AND PROBLEM

In this project, a rainy condition lane detection video has been used, which differs from standard lane detection databases. It presents additional challenges, including rain on the windshield and frequent windshield-wiper motion, which obstructs lane lines and triggers incorrect detections. Rain on road surfaces, as well as on the windshield, along with reflections, increases the challenge for detection by making it difficult for standard lane detection methods to function properly. The dataset considered in this experiment is very different from other lane detection cases because of some challenges. The major challenge in this experiment is wiper interference because wipers move back and forth in the field of view of a camera, which leads to wrong detections. Standard lane detection methods are not effective in such scenarios because wipers cast temporary blind spots, which mislead edge detection and feature-extraction techniques. The second challenge is the occurrence of rain on the windshield, which degrades frames captured by a camera by adding noise. Low visibility because of rain reduces contrast between lanes on the ground and the road, which makes lane boundary detection very challenging. In addition, reflections from headlights, wet surfaces and wet wipers contribute to fluctuating intensity values, which further hinder the performance of edge-based lane detection techniques.

Initially, a normal sliding window and Hough Transform approach was implemented for lane detection to distinguish between the results from a normal approach and the proposed solutions. The sliding window approach is the first approach that has been adopted, and it involves various steps. The first step in the flow is reading the video and selecting the region of interest. ROI is selected to exclude irrelevant background and focus on the lane in the bottom half of the image where lane markings are likely to be

present. It is selected by using four coordinates placed in the form of a trapezoid, as shown in Figure 1(a), where tl, bl, tr and br refer to the top-left, bottom-left, top-right, and bottom-right, respectively.

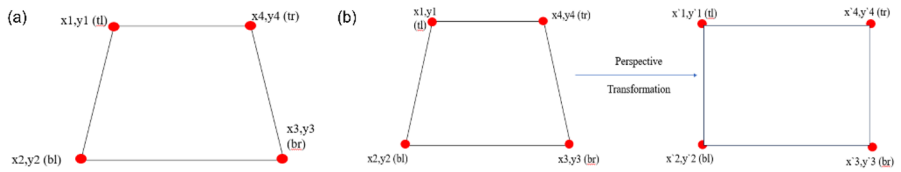

Fig. 1. (a)Schematic form of a Region of Interest as a Trapezoid (b)Perspective transformation of ROI

After selecting the ROI, Perspective Transformation is conducted to obtain a bird's-eye view of the highway. Four points in the original image corresponding to the positions of the lanes are then converted to new points where the lanes are parallel, as shown in Figure 1(b). After perspective transformation, image thresholding is executed. The background is transformed into low-intensity values (black), while lane markings are highlighted as high-intensity values (white). Now, a histogram-based method is used to identify peak intensity values in the lower half of the frame, which correspond to the lane positions. Since multiple peaks may be observed in the histogram, the two most prominent peaks, representing the left and right lanes, are selected, while other peaks are discarded as noise. Rectangular windows are then placed iteratively along the vertical axis to track the lane boundaries. The centroid of each rectangular window is adjusted using the OpenCV function cv2.moments, ensuring that the windows shift by lane movements. This iterative adjustment allows for robust tracking of lane boundaries, even in the presence of slight shifts due to vehicle motion. After lane boundary points are extracted using the sliding window approach, the lane boundary visualisation step is performed. Before proceeding, the continuity of lane points is verified using previous frames to ensure stability in lane tracking. Once continuity is established, a quadrilateral is formed, which represents the lane, and a green-colored polygon is overlaid onto the bird's-eye view to highlight the detected lane [6]. To present the detected lane markings in the original camera view, an inverse perspective transformation is applied, mapping the detected lanes back onto the original frame. Further, the accuracy is calculated in the form of IOU using the CVAT Annotation tool to create annotations where manual annotations are created, and .xml file is generated, which is further used to generate ground truth masks with the help of a MATLAB code [7]. The annotated ground truth frames and further compared with the detected frames for calculating the IOU. Further, Frames Per Second (FPS) is also measured to assess real-time processing capability, which is calculated as the number of frames processed in a second [8]. The IOU calculated using this method was 58.47%, with a frame rate of 3.99. The frames in which the lane gets detected accurately can be seen in Figure 2(a). However, there were some frames in which the sharp edges of the wiper were detected as lanes, leading to false detection and hence reducing the IOU. The wrongly detected frames can be seen in Figures 2(b), 2(c), and 2(d). Also, in figure 2(e), the left lane is not visible in

the frame due to which it considers the edge of wiper and provides the lane path accordingly, in figure 2(f), lane is clearly visible and sharp edge of the wiper is also interfering a little bit, but the lane is detected accurately as it considers the lane line and not the sharp edge of the wiper. However, if the influence of the wiper in this frame was more, the lane would be wrongly detected even if the white lane was visible, which can be seen in Figure 2(g). A Graphical representation is used to analyse the IOU across different frames in Figure 3, which shows the IOU using the sliding window (SW) method. The IOU values fluctuate significantly in the early frames, with sharp drops and sudden recoveries, suggesting that the method struggles with consistency. The flow diagram of this whole process is shown in Figure 4 below.

Fig. 2. (a)The frame of which the lane lines get detected correctly (b)The frame of which the wiper is wrongly detected as the lane border (c)Frame showing the edge of the wiper getting detected (d)Frame showing the edge of the wiper getting detected (e)The left lane is faded in this frame, and the edge of the wiper gets detected (f)Both the wiper's edge and the left lane are visible, but the lane is still detected accurately in this frame (g)This frame shows the influence of the wiper more, due to which edge of the wiper gets detected

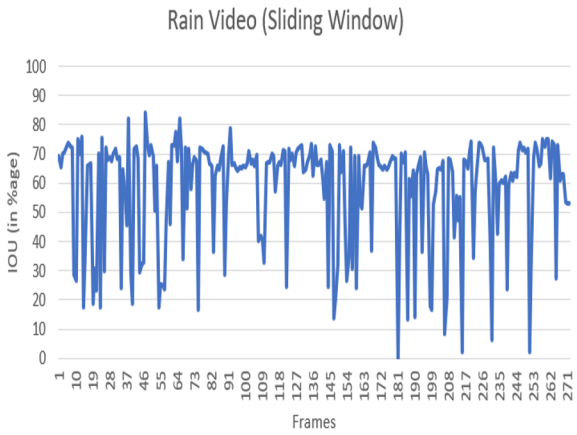

Fig. 3. Graphical representation of IOU over different frames using SW

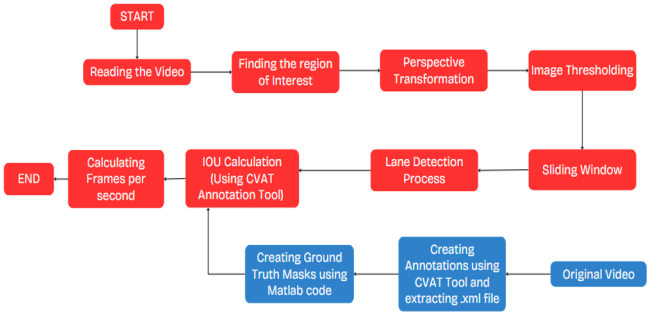

Fig. 4. This flow diagram shows the process flow using the SW Approach

Another approach used in this study is the Hough Transform, which is well-suited for detecting straight or slightly curved lane lines. The process begins by reading the video and resizing each frame to a 640×480 resolution. Once the frames are obtained, Canny Edge Detection is applied to highlight lane edges. There are three main steps in Canny: conversion of the frame to grayscale, Gaussian Blurring of the image to remove noisy edges, and edge detection by calling OpenCV's cv2.Canny() function on thresholds (50, 150) [9]. Edges lower than 50 are ignored, and edges 150 or higher are considered strong edges. After edge-detected frames, the Region of Interest (ROI) is chosen to separate lane markings. Finally, the application of the Hough Transform is done, in which the edge pixels are converted to Hough space to identify parallel points that constitute lane lines. Detected lines are then converted back to the original frame. Further, the iou is computed using the CVAT annotation tool for creating annotations in the original video and downloading the .xml file to use it in the MATLAB code for generating ground truth masks and comparing them with the detected frames using the algorithm. The iou computed using the Hough Transform was 16.53% with a frame rate of 10.21. However, only some frames were correctly detected, which can be seen in Figure 5(a). As the Hough transform is known to detect straight lines, it can be seen in other frames in Figures 5(b), 5(c), 5(d) and 5(e), where the algorithm is detecting the

wiper as a straight line, further reducing the iou. Further, a graphical representation of iou over different frames is analysed in Figure 6, which illustrates the IOU performance of the Hough Transform (HT) method under similar conditions. The flowchart of the Hough Transform Approach can be seen in Figure 7 below. Compared to the SW method, the IOU values for HT remain low, with frequent drops to near zero. The sheer number of frames of near-zero IOU means that the HT approach is considerably sensitive to wiper occlusions, causing lane detection to fail frequently. It implies that the HT approach is unable to ensure consistent lane observability in the presence of dynamic occlusions such as windshield wipers.

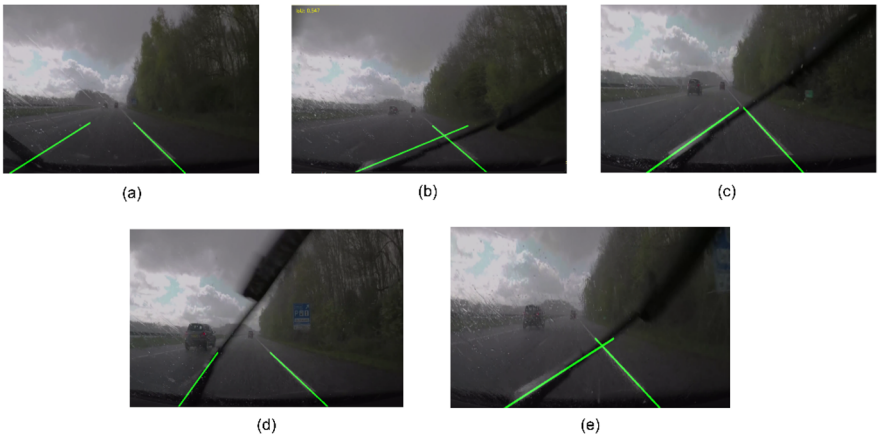

Fig. 5. (a)The Frame in this figure shows the correct detection of lane lines (b), (c), (d), € The frame in this figure detects the wiper's edge as the left lane line.

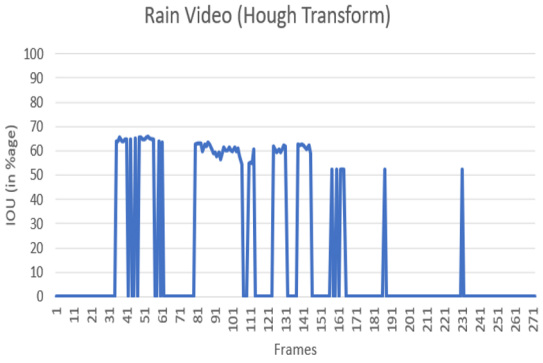

Fig. 6. Graphical representation of IOU over different frames using the HT Approach

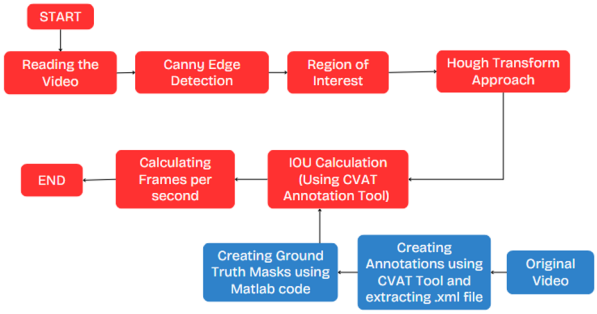

Fig. 7. This flow diagram shows the process flow using the HT Approach

3 PROPOSED SOLUTION

A. Solution using Sliding Window Approach

In this enhanced solution, a sliding window method is used to streamline and improve lane detection. In contrast to the original solution, which depended upon extensive use of morphological operations and adaptive thresholding, this solution prevents excessive preprocessing that might interfere with lane visibility. Firstly, the mask preprocessing step in Code2 uses a stronger morphological closing (2 iterations) and a larger Gaussian blur kernel (5x5) to better suppress noise caused by rain and windshield wipers. It also removes the adaptive thresholding, which, although effective in some cases, can amplify noise and result in fragmented lane detections under varying illumination. The other important enhancement lies in the loop structure; the original solution processed the left and right lanes separately in two different loops with redundant processing and higher computation. The latest solution processes both lanes together in one loop, resulting in fewer iterations, more optimal execution, and cleaner processing. The maximum IOU recorded in this case was 73.72%, and the minimum IOU recorded was 0.1%, and the frames for these IOU values are shown in Figures 8(a) and 8(b), respectively. However, the average IOU recorded was 64.62% with a frame rate of 5.88 per second.

(a) (b)

Fig. 8. (a)The frame in this figure shows the maximum IOU of 73.72% (b)The frame in this figure shows the minimum IOU of 0.1%

B. Solutions using the HT Approach

1) First Solution using HT Approach

The HT algorithm was subsequently improved by a series of experimental modifications, enhancing the identification of lanes in rainy conditions. Three scenarios were investigated to deal with rainy weather conditions, and enhancements of the edge detection and the related preprocessing processes were included in each of them.

Case (i): Tuning the Canny Edge Detection Thresholds

During the initial implementation, the Canny Edge Detection was applied using the thresholds of (50,150). These thresholds are generally good at identifying strong edges, but in this case, the set of high thresholds caused the detection of strong, unwanted edges like the windshield wipers. These detections had the unintended consequence of causing frequent misclassification of the wiper edges as lane lines. To address this problem, the thresholds of the Canny were lowered to (30,50). By reducing the threshold values, the algorithm became more effective at identifying weak edges, specifically, the edges of the lane lines, which were not so strong due to the effects of rain. This adjustment considerably diminished the detections caused by the wipers and enhanced the detection of the left lane, which had previously gone undetected in many of the input frames due to its weak edges. The maximum IOU after implementing case(i) was 96.46%, and the respective frame can be seen in Figure 9(a) below. It can be observed that even with the interference of the wipers, the lane lines are detected accurately, whereas the lowest IOU value observed was 0% which is shown in Figure 9(b) which is the first frame of the video where only the right lane gets detected and it takes a while for the left lane to get detected. The average calculated IOU was estimated as 73% with a frame rate per second as 7.14.

(a) (b)

Fig. 9. (a)The frame in this figure shows the maximum IOU of 96.46% (b)The frame in this figure is the first frame and it shows the minimum IOU of 0%

Case (ii): Use of CLAHE for contrast

In this case, the CLAHE was implemented in every frame before processing it using the Hough Transform and the Canny Edge Detection. CLAHE is a sophisticated method of enhancing the visibility of image features by utilizing localized equalization. It lowers the contrast of rain conditions and makes lane markings and road surfaces difficult

to discern. By using CLAHE, the visual clarity of the frames was enhanced, and lane markings were viewed more sharply. It improved the performance of the Canny Edge Detection and enhanced the precision of the subsequent Hough line detection due to the enhanced contrast. The maximum IOU after implementing this case was 96.36%, and the respective frame can be seen in Figure 10(a) whereas the minimum IOU in this case was 0% which is the first frame of the video in which the right lane gets detected but left lane takes a while to get detected which can be seen in the Figure 10(b) below. The average calculated IOU was estimated as 70.43% with a frame rate of 4.45 per second.

(a) (b)

Fig. 10. (a) The frame in this figure shows the maximum IOU of 96.36% (b)The frame in this figure is the first frame and it shows the minimum IOU of 0%

Case (iii): Combination of Modified Canny Thresholding and CLAHE

This case comprised a fusion of the improvements of the preceding two scenarios. This hybrid solution commenced by enhancing the contrast using CLAHE and then proceeded to use the modified low thresholds (30,50) in the subsequent Canny Edge Detection. This combined method showed enhanced robustness and precision in unfavorable weather conditions. The maximum IOU recorded in this case was 96.9%, which is approximately 97%, and the minimum IOU was 3.31%, and the respective frames can be seen in figures 11(a) and 11(b), respectively. The average IOU for all the frames was estimated as 76.8% with a frame rate of 9.34 per second. Also, it was observed in the previous two cases that the first frame of both cases showed an IOU of 0% because of the left lane not getting detected, whereas in this case, the first frame showed an IOU of 86.69% and the respective frame is shown in Figure 11(c).

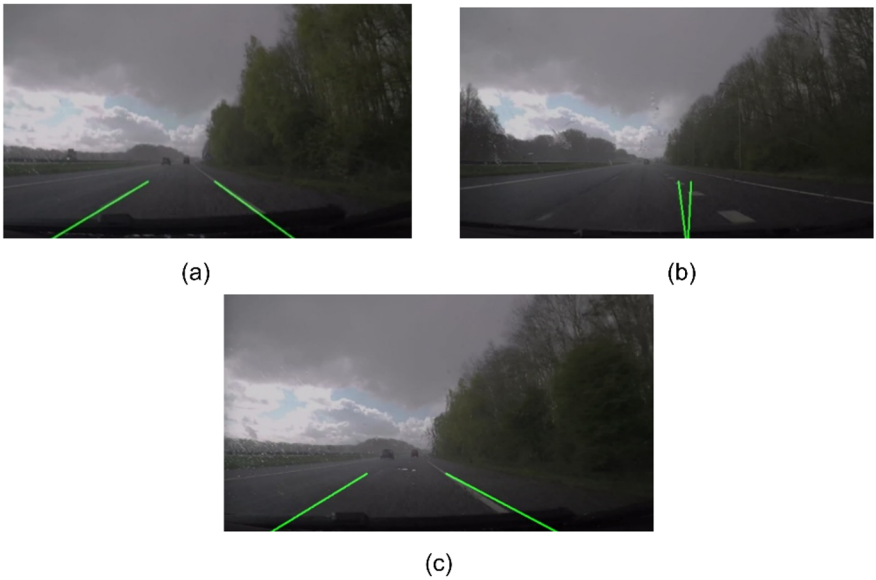

Fig. 11. (a)The frame in this figure shows the maximum IOU of 96.9% (b)The frame in this figure shows the minimum IOU of 3.31% (c)The frame in this figure is the first frame of the video, which showed an IOU of 86.69%

2) Second solution using HT

In the previous method utilizing the Hough Transform technique, both a low Canny edge detection threshold of (30, 50) and CLAHE were applied to increase the visibility and difference of edges in the rain scenario. This method, however, depended on global thresholding, in which a single cutoff threshold is applied to the whole image. This drawback caused the method to be less effective in scenarios where there is a change of environmental illumination and rain-reflection-induced noise. In the second solution, Adaptive Thresholding is applied before the use of the Canny edge detection, which adjusts the threshold value dynamically per region based on the intensities of the neighboring pixels [10]. In contrast to the use of a constant threshold applied to the entire image in fixed thresholding, adaptive thresholding calculates different thresholds per region of the image. This is highly effective in dynamically illuminated scenes, such as rain scenarios, in which the localized differences in brightness and contrast can confuse global threshold values. The method of adaptive threshold uses the method of subdividing the grey-scale image into small matrices of size 3×3 pixels. For every matrix, the average of the matrix is calculated, and the matrix average is used as the binarization boundary value. Pixel intensities above the local average are converted to white (255), while intensities below the average are converted to black (0). This localized processing method preserves lane lines, even when illumination varies in the frame due to rain, illumination by the reflections from the road or wipers. An example illustration of this

method is given in Figure 12(a), where a 3×3 matrix located in the center of a large block of the image is binarized using its local mean of 122, resulting in a well-matched binary mask, where values greater than 122 are converted to high intensity value (255) and values less than 122 are converted to low intensity values (0).

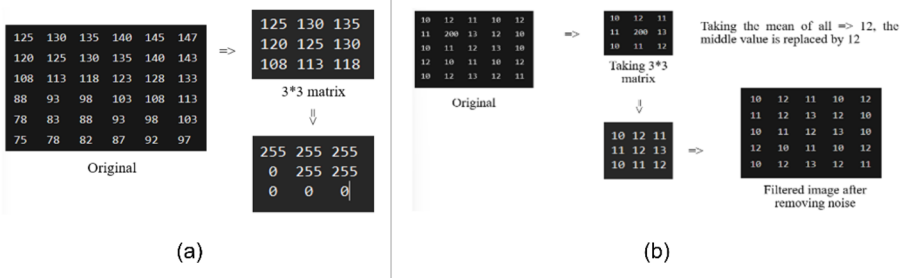

Fig. 12. (a)An example matrix of how adaptive thresholding works (b)An example matrix of how Median Filtering works

In addition to adaptive thresholding, the improved method integrates Median Filtering before thresholding [11]. By replacing the pixel value of the noise with the median of its neighboring pixels, abrupt intensity changes that are not part of the actual lane structure are smoothed out without blurring the edges of the lane lines. An illustration of this concept is shown in an example in Figure 12(b), where a 3×3 matrix centred within a larger intensity value at the center, i.e. noise, is replaced by the mean value of 12, resulting in a well-adapted binary mask. In addition, the slope-based filtering conditions are applied, due to which the Hough Transform have also been improved. In the past, the lines were categorized as being part of the left or the right lane using fixed slope boundaries (for example, slopes below -0.3 for the left and above 0.3 for the right). We noticed, though, that more relaxed constraints on the slope enabled unwanted lane features like wiper streaks or reflections to be incorrectly labelled as lanes. In this enhanced version, the slope criterion in the detection of the right lane is tightened (to slope > 0.85), strongly avoiding the detection of spurious lines by only admitting lines having a sharp inclination to the right. These enhancements together serve to increase the Hough Transform method's robustness in rain conditions. Adaptive thresholding and median filtering aid in a purer edge map, enabling the Hough Transform to concentrate more on structurally significant details. The maximum IOU observed in this case was 84.25%, whereas the minimum IOU for this proposed solution was 61.38%, which can be seen in Figures 13(a) and 13(b), respectively. Moreover, the average IOU computed using this method was 73.43% with a frame rate of 7.7 per second.

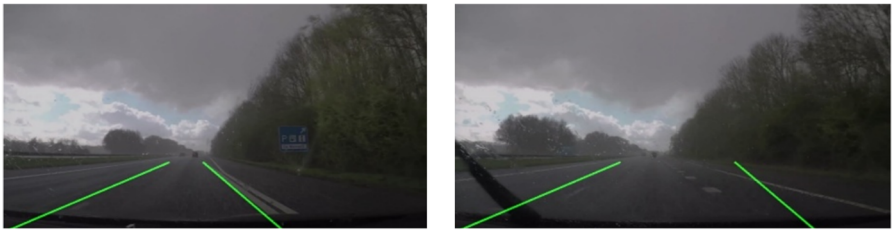

(a) (b)

Fig. 13. (a)The frame in this figure shows the maximum IOU of 84.25% (b)The frame in this figure shows the minimum IOU of 61.38%

4 RESULTS AND COMPARISON

A. Results using Sliding Window

To evaluate the robustness of the Sliding Window Approach under rainy conditions, a comparative analysis of various solutions was performed on a test video. Initially, the basic Sliding Window Approach was applied without any modifications. As it can be seen in Figure 14(a), the majority of frames have IOU values clustered around 70 and 80, with the 70range having the highest frame count at over 100 frames, and the 80 range at about 70 frames. Lower IOU values (10–60) also have some presence, but with much fewer frames. This distribution illustrates that the number of frames having 0 IOU will be counted in the 0 numbered bin, frames having IOU greater than 0 and less than 10 will be counted under 10 frequency bin, frames having IOU less than 100 and greater than 90 will be counted in 100 frequency bin, and so on. However, the average IOU is typically lower because of some factors like the water droplets of the rain on the camera lens reduce clarity, making it harder for the model to detect the lanes accurately, leading to poor visibility, Fast falling Raindrops cause motion blur, making it difficult to precisely detect the lanes, and Water droplets on the camera lens distort the image, leading to incorrect segmentation and reduced IOU scores. Rainy conditions often result in low-contrast images, making the lane boundaries harder to distinguish. Another reason for low IOU is the presence of the car wipers in use, due to which the camera view gets blocked, which hides the lane lines in between. These factors cause the predicted mask to deviate more from the ground truth mask, reducing the IOU.

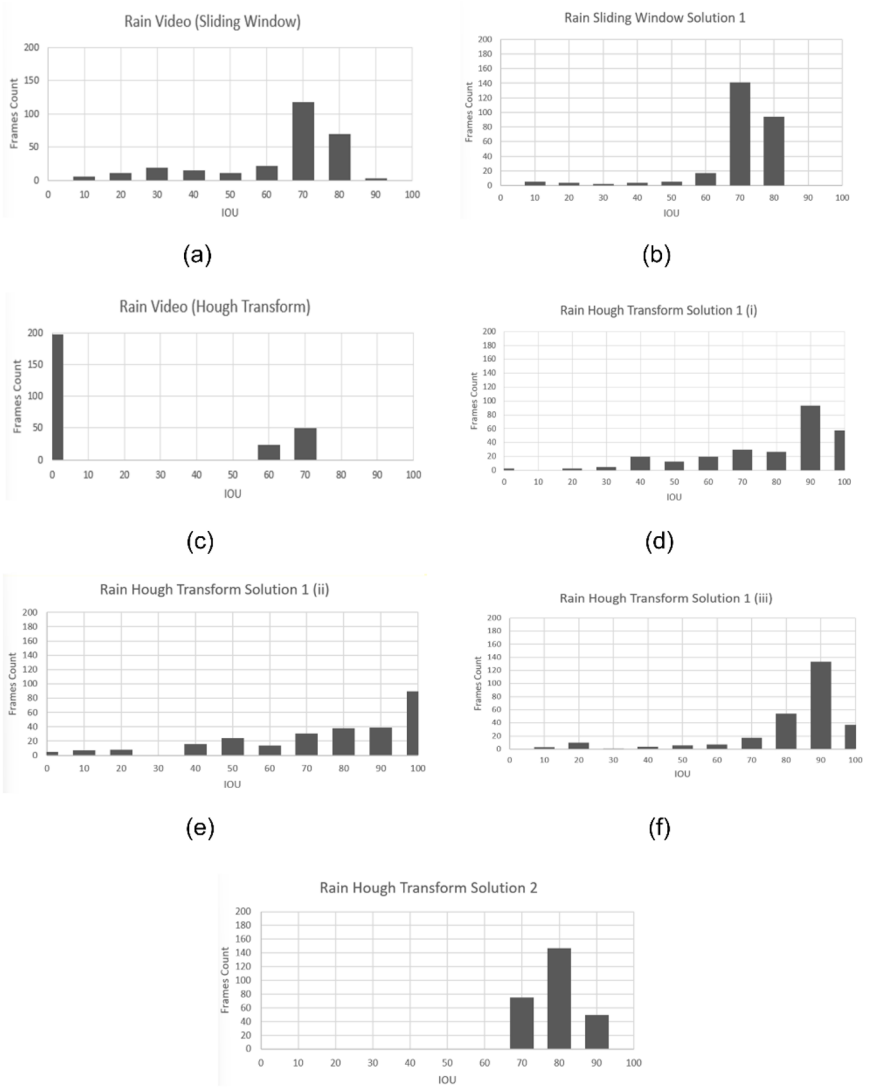

Fig. 14. (a)Graphical distribution of the total frame count over different IOU values using SW Approach (b)Graphical distribution of total frame count over different IOU values using the SW Approach (c)Graphical distribution of total frame count over different IOU values using the HT (d)Graphical distribution of total frame count for different IOU values using the HT case(i) (e)Graphical distribution of total frame count for different IOU values using the HT case(ii) (f)Graphical distribution of total frame count for different IOU values using the HT case(iii) (g)Graphical distribution of total frame count for different IOU values using the HT Approach

To address this issue, some improvements were made to the initial implementation. In this enhanced solution, a sliding window method is used to streamline and improve lane detection. In contrast to the original solution, which depended upon extensive use of morphological operations and adaptive thresholding, this solution prevents excessive preprocessing that might interfere with lane visibility. The mask preprocessing step in this code uses a stronger morphological closing (2 iterations) and a larger Gaussian blur kernel (5×5) to better suppress noise caused by rain and windshield wipers. It also removes the adaptive thresholding, which, although effective in some cases, can amplify noise and result in fragmented lane detections under varying illumination. The effectiveness of the enhanced approach is reflected in the evaluation metrics. The maximum IOU recorded was 73.72%, and the minimum was 0.1%. Despite the challenging conditions, the method achieved an average IOU of 64.62%, maintaining a frame rate of 5.88 frames per second. It can be observed in Figure 15(a) that for most of the frames, the IOU remains relatively stable between 65% and 75%, suggesting consistent and accurate detection performance across the video. However, starting around frame 170, the graph exhibits significant drops in IOU values, with some frames reaching very low scores close to 0%. These fluctuations indicate that the algorithm struggles with detection accuracy in specific sections of the video, possibly due to changes in lighting or heavy rain intensity. Despite these, it demonstrates that the solution maintains reasonably good performance across a majority of frames. It can be seen in Figure 14(b) that the majority of frames achieved high IOU values, particularly around 70 and 80, with approximately 140 and 90 frames, respectively. In contrast, very few frames recorded lower IOU values, such as 10, 20, 30, 40, 50, and 60, each contributing only a small number of frames. This distribution suggests that the Sliding Window approach is stable, successfully achieving accurate detections in most frames.

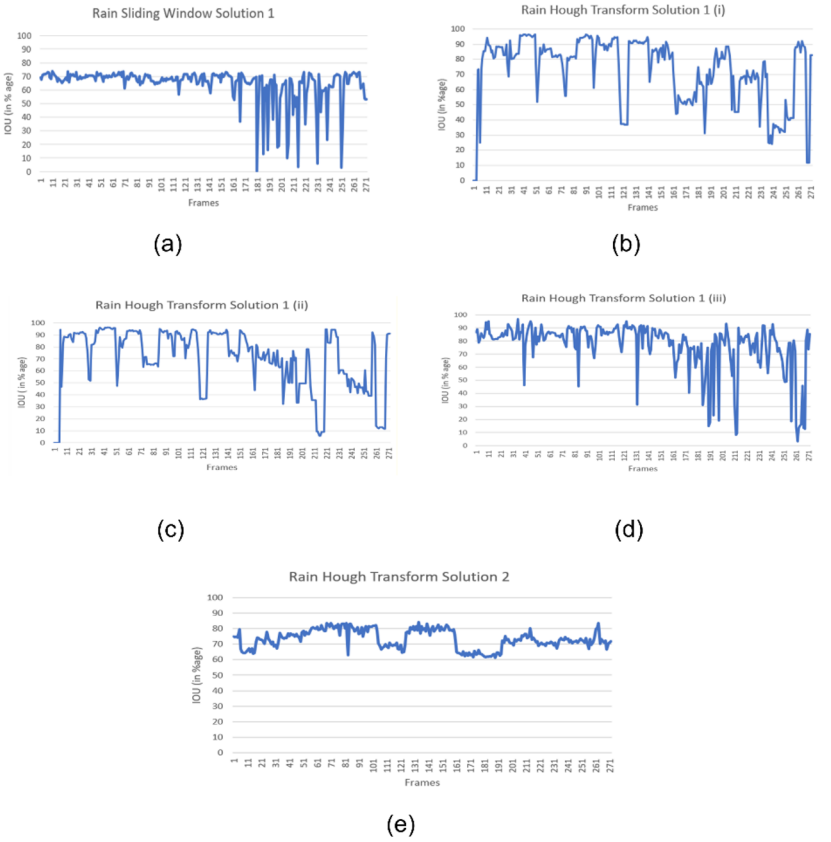

Fig. 15. (a)Graphical representation of IOU over different frames using the SW Approach (b)Graphical representation of IOU values for different frames using the HT case(i) (c)Graphical representation of IOU values for different frames using the HT case(ii) (d)Graphical representation of IOU values for different frames using the HT case(iii) (e)Graphical representation of IOU values over different frames using the HT Approach

B. Results Using Hough Transform

A comparative analysis of various solutions was performed on a test video to evaluate the robustness of the Hough Transform under rainy conditions. Initially, the basic Hough Transform was applied without any modifications. As seen in Figure 14(c), a significant number of frames yielded inferior detection results, with IOU values clustering near zero. The bar chart indicates that nearly 200 frames had IOU values below 10%, confirming that the baseline method is ineffective in rainy scenarios. This is primarily due to the presence of visual obstructions like raindrops, reflections, and windshield wipers, which distort or suppress the visibility of lane lines. To address this, a

first set of improvements was introduced in the form of three sub-cases under Hough Transform Solution 1. These cases involved case(i) of adjusting Canny edge detection thresholds from (50, 150) to (30, 50), case(ii) enhancing contrast using CLAHE and case(iii) combining both techniques. The line graphs of these three cases in Figs 15(b), 15(c) and 15(d) show considerable improvement in IOU values as compared to the baseline. Cases (i) and (ii) have relatively stable IOU values in the greater part of the frames, along with occasional drops owing to potentially heavier rain streaks or occasional obstacles. Case (iii), which integrates the two improvements, shows the highest and most stable IOU performance in parts of the video sequence but also frequent drops, indicating that although the detection is more crisp, it can remain susceptible to sharp distortions due to moving wipers or heavy rain droplets. It can also be observed that the graph for case(i) shows a stable pattern with high accuracy in the early frames. However, there are sharp dips in certain frames, such as frame 121 in Figure 15(b), where the IOU falls significantly. This drop is mirrored in the Case (ii) graph in Figure 15(c), which uses CLAHE enhancement, indicating that both methods still suffer from certain visual obstructions like wipers or dense rain. In contrast, the Case (iii) graph shows a much smaller dip at frame 121, demonstrating better resilience to sudden distortions.

A graphical distribution of the above three cases can be seen in the three figures below in the form of a histogram, where the horizontal axis shows the IOU values and the vertical axis provides the frame count. It is observed from the first graph in Figure 14(d) that the highest concentration of frames occurs at 90 IOU (~95 frames) and 100 IOU (~60 frames), with moderate distribution across mid-range IOU values (40–70). In comparison, the second plot in Figure 14(e) shows a peak of about 90 IOU. On the other hand, the third plot in Figure 14(f) indicates a steep peak at 90 IOU with around 130 frames, a secondary peak at 80 IOU (about 50 frames), and a moderate value at 100 IOU (about 35 frames). It also indicates low counts of frames at low IOU values, pointing towards focused detection at around 90 IOU. In general, the third solution indicates a high concentration of high accuracy.

The second solution of the Hough Transform incorporated adaptive thresholding and median filtering before applying Canny edge detection. This approach yielded significantly more consistent and reliable results across the entire video sequence, as seen in Figure 15(e). The IOU values now predominantly range between 65% and 85%, with only minor fluctuations. The use of adaptive thresholding dynamically adjusted to varying lighting and visibility conditions, ensuring better lane segmentation even during transient occlusions. Meanwhile, median filtering played a crucial role in mitigating the impact of transient noise, such as raindrops and wiper movements, by preserving lane structures while removing outlier artefacts. Here, overall, all the IOU values are quite consistent, being predominantly in the range of 70% to 80%, signifying steady performance. In the first part of the segment (frames 1–80), IOU fluctuates from 65% to 80% with moderate but unstable detection. In frames 81 to 160, the model exhibits more consistent performance with IOU values predominantly exceeding 75%, although there

are periodic dips. There is a sharp drop in frames 160 to 190, where IOU is in the range of 60–65%, which is indicative of poor performance. This then develops into a pick-up in frames 191 to 230, where IOU again increases to the range of 70–80%. In the later segment of 231 to 271, performance decreases marginally again but is in a steady range with random spikes to nearly 90%. Compared to Solution 1 variations, Solution 2 provides more frame-to-frame consistency but lacks the higher IOU concentration, particularly in the 90–100% range, making it more stable but less precise in peak detection accuracy. Also, the graphical distribution is shown in Figure 35 using a histogram, where it can be seen that most frames have an IOU between 70% and 90%, indicating that the solution generally performs within a reliable accuracy range. Specifically, the highest number of frames, around 145, fall within the 80% IOU bin, demonstrating strong detection consistency. This is followed by approximately 75 frames in the 70% IOU and around 50 frames in the 90% IOU bin. There are no frames in the lower IOU ranges (below 70%), confirming that the solution avoids poor detections and maintains a relatively high baseline performance. Compared to the individual fluctuations seen in the line graph, this histogram confirms that Solution 2 consistently maintains good IOU values for the majority of frames.

C. Comparison of the results from both methods

To analyse how effective both SW and HT approaches would be in rainy weather, IOU was used as the main metric among different solution variants. The improved SW method reached an average of 64.62% IOU, and the frames were mostly clumped around 70–80% IOU. The performance, though, dropped significantly beyond frame 170, where IOU dramatically declined due to unfavorable weather artefacts like motion blur and water drops. The highest peaks were reached by HT Solution 1 (combination of CLAHE + adjustments to Canny) with 130+ frames at 90% IOU, and a secondary peak at 80%. HT Solution 2 maintained a more consistent performance, with over 145 frames falling in the 80% IOU range, despite fewer extremely high IOU scores. SW Approach Demonstrated a bell-curve-like IOU distribution, where the highest frame counts were in the 70 and 80 bins (~140 and ~90 frames, respectively). The low IOU bins (10–60) exhibited low frequency, reflecting strong mid-ranged performance but susceptibility to drastic distortions. Nonetheless, both HT Case (i) and (ii) exhibited moderate advance relative to baseline but sustained steep drops at particular frames. HT Case (iii) generated a focused peak at 90 IOU (~130 frames) and reflected high accuracy with intermittent inconsistency. HT Solution 2 generated an even distribution between 70–90 IOU, validating stable and consistent detection throughout the video.

D. Discussion

The SW Approach would be optimal in cases needing moderate computing capabilities, as SW can be less resource-consuming than highly complex HT pipelines. Where there is anticipated short duration rain or light distortion, and frame rate is of higher concern

(to achieve ~5.88 FPS). It is effective when lane visibility is relatively consistent, and its enhanced version reduces preprocessing complexity while improving robustness. However, it is less resilient to heavy rain, fast wiper motion, and camera lens obstruction, which is seen in the case where the IOU drops significantly in later video frames under intense rain. HT Approach is best suited for Heavy rain scenarios or frequent occlusions, where visibility of lane lines is poor or rapidly changing and real-time road assistance systems that prioritize consistent lane detection over raw frame speed. HT Solution 2 provided the most stable and high-performing detection, with over 90% of frames above 70 IOU, and Adaptive thresholding and median filtering dynamically respond to lighting and noise variations. But in Solution 1, notwithstanding that some of these variants (such as case iii) have high peak accuracy, they experience sudden drops due to steep distortions. The HT (particularly Solution 2) is superior to SW regarding stability, robustness, and detection quality in adverse weather such as rain and occlusion. However, the SW solution is still useful in benign weather or resource-scarce environments because of its less complex structure and comparatively quicker frame processing.

5 FUTURE PERSPECTIVES

While the solutions presented in this study have demonstrated encouraging performance for rainy scenarios and windshield wiper interference, several areas are left for future investigation and improvement. Firstly, the creation of an all-encompassing dataset that encompasses diverse rainy scenarios involving multiple wiper speeds, angles, and types of vehicles would allow for more robust tuning of algorithms. Such a dataset would also allow effective use of machine learning models trained specifically to detect and eliminate the patterns created by strokes from wipers. Second, using temporal filtering techniques, such as differencing frames, temporal median filtering, or motion separation using optical flow, can further enhance the robustness of detection by tracking robust lane structures from one frame to the next and discarding transitory occlusions. This would be especially useful for instances where lane markings are momentarily occluded due to heavy rain or very high-speed wiper movement. Third, one may investigate sensor fusion strategies incorporating vision and Lidar or radar data for verification and support of lane detections. While vision is vulnerable to image noise, other sensor modalities may provide complementary information that is immune to surface reflection or rain streaks. Fourth, application of learning methods where the system adapts the detection parameters from time-stamped and motion information can generalize the approach to other adverse conditions like snow or fog or nighttime glare. The suggested changes to traditional vision-based lane detection methods represent a solid platform for more advanced and scalable approaches to autonomous driving under bad weather and future exploration of robustness and adaptability.

6 CONCLUSION

This study pays particular attention to an important and yet largely understudied problem of vision-based lane detection under the interference brought about by the use of windshield wipers in rainy conditions. Traditional lane detection techniques, such as Sliding Window and Hough Transform, perform admirably well on ideal driving scenarios. But their performance is radically heightened if they are subjected to rain-induced noise and wiper-induced occlusion dynamics. Using a series of systematic augmentations, such as adaptive thresholding, median filtering, slope constraints that act dynamically, and using CLAHE for contrast enhancement, this research introduces an improved, robust approach that maintains lane detection precision even in the worst conditions. Experimental tests carried out by this research show noteworthy gains in both IOU and lane detection consistency across frames compared to baseline approaches. By comparing traditional methods such as Sliding Window and Hough Transform, both with and without the respective augmentations, it may be realized that the proposed changes significantly enhance lane recognition precision, particularly in rain and wiper interference-affected frames. The enhancing factors are due to the addition of adaptive thresholding, median filtering, and improved geometric constraints, all of which combine to enhance edge clarity and eliminate false positives. The comparison also reveals an important observation, that while the edges of wipers commonly replicate lane shape and contrast, these may efficiently be distinguished and eliminated using contextual and slope-based information, and by checking line continuity between frames. This allows the system to maintain focus on persistent lane structures while ignoring transient, motion-induced noise. As a result, the refined classical algorithms presented in this work serve as a computationally efficient alternative, making them particularly well-suited for real-time deployment on embedded automotive platforms, where resource constraints are critical.

References

1. N. J. Zakaria *et al.*, "Lane Detection in Autonomous Vehicles: A Systematic Review," *IEEE Access*, vol. 11, pp. 3729–3765, 2023, doi: 10.1109/ACCESS.2023.3234442.
2. N. U. A. Tahir *et al.*, "Object Detection in Autonomous Vehicles under Adverse Weather: A Review of Traditional and Deep Learning Approaches," *Algorithms*, vol. 17, no. 3, Art. no. 103, 2024, doi: 10.3390/a17030103.
3. J. N. Morden, F. Caraffini, I. Kypraios, A. H. Al-Bayatti, and R. Smith, "Driving in the Rain: A Survey toward Visibility Estimation through Windshields," *Int. J. Intell. Syst.*, 2023, doi: 10.1155/2023/9939174.
4. J.-Q. Zhang, H.-B. Duan, J.-L. Chen, A. Shamir, and M. Wang, "HoughLaneNet: Lane detection with deep hough transform and dynamic convolution," *Comput. Graph.*, vol. 116, pp. 82–92, 2023, doi: 10.1016/j.cag.2023.08.012.
5. S. Kumar, M. Jailia, and S. Varshney, "An efficient approach for highway lane detection based on the Hough transform and Kalman filter," *Innov. Infrastruct. Solut.*, vol. 7, Art. no. 290, 2022, doi: 10.1007/s41062-022-00887-9.
6. S. Shabani, J. Ayoubinejad, and N. B. Rahmanian, "Identification of Road Black Spots Based on the Sliding Window Optimization and Safety Performance Function Development," *Baltic J. Road Bridge Eng.*, vol. 19, no. 1, pp. 88–113, 2024, doi: 10.7250/bjrbe.2024-19.629.

7. P. Sadeghi and A. Goli, "Investigating the impact of pavement condition and weather characteristics on road accidents," *Int. J. Crashworthiness*, vol. 29, no. 6, pp. 973–989, 2024, doi: 10.1080/13588265.2024.2348269.
8. S.-H. Lee, H.-J. Kwon, and S.-H. Lee, "Enhancing Lane-Tracking Performance in Challenging Driving Environments through Parameter Optimization and a Restriction System," *Appl. Sci.*, vol. 13, no. 16, Art. no. 9313, 2023, doi: 10.3390/app13169313.
9. S. Samantaray, R. Deotale, and C. L. Chowdhary, "Lane Detection Using Sliding Window for Intelligent Ground Vehicle Challenge," in *Lecture Notes on Data Engineering and Communications Technologies*, Singapore: Springer, 2021, pp. 871–881, doi: 10.1007/978-981-15-9651-3_70.
10. D. J. Pangal *et al.*, "A Guide to Annotation of Neurosurgical Intraoperative Video for Machine Learning Analysis and Computer Vision," *World Neurosurg.*, vol. 150, pp. 26–30, 2021, doi: 10.1016/j.wneu.2021.03.022.
11. J. Wang *et al.*, "Effect of Frame Rate on User Experience, Performance, and Simulator Sickness in Virtual Reality," *IEEE Trans. Vis. Comput. Graph.*, vol. 29, no. 5, pp. 2478–2488, 2023, doi: 10.1109/tvcg.2023.3247057.
12. A. Lapušinskij *et al.*, "The Application of Hough Transform and Canny Edge Detector Methods for the Visual Detection of Cumuliform Clouds," *Sensors*, vol. 21, no. 17, Art. no. 5821, 2021, doi: 10.3390/s21175821.

.